

Original Article

# Effect of Base Thickness on the Performance of a Polycrystalline Silicon-Based Semiconductor Radial N/P Junction Solar Cell in the Static Regime under Monochromatic Illumination

Aboubacar Savadogo<sup>1</sup>, Bernard Zouma<sup>1</sup>, Ramatou Konate<sup>1,2\*</sup>, Cyrille Constant Moyenga<sup>1</sup>, Raguilignaba Sam<sup>3</sup>

<sup>1</sup>Department of physic, Laboratoire d' Energies Thermiques RENouvelables(L.E.T.RE),  
Université Joseph KI-ZERBO/Ouagadougou, Burkina Faso.

<sup>2</sup>Université virtuelle du Burkina Faso /Ouagadougou, Burkina Faso.

<sup>3</sup>Department of Physic, Université Nazi Boni/ Bobo Dioulasso, Burkina Faso.

\*Corresponding Author : korama\_ms@yahoo.fr

Received: 09 October 2023

Revised: 28 November 2023

Accepted: 15 December 2023

Published: 30 December 2023

**Abstract** - In this work, the importance of the base thickness on the performances of a radial n/p junction solar cell-based polycrystalline silicone is shown. Thus, from a theoretical study under monochromatic illumination in a static regime, we established new analytical expressions of electrical parameters. By simulations on Mathcad 15 software with photocurrent-photovoltage (J/V) and power-photovoltage (P/V) characteristics, we were able to extract the numerical values of maximum power, photovoltage, photocurrent, short-circuit photocurrent, the open-circuit photovoltage, fill factor, optimum load resistance and conversion efficiency ( $\eta$ ) for different thicknesses of the base. The analysis clearly shows that unlike the resistance, which decreases, the other parameter values increase with the increase of the base thickness. The short circuit photocurrent density ( $J_{phcc}$ ) is more sensitive to the thickness  $H$ , with an increase of 87% observed. When  $H$  increases from 30 to 150  $\mu\text{m}$ , the  $J_{phcc}$  goes from 21.989 to 41.161  $\text{mA}/\text{cm}^2$ . This leads to an improvement in the efficiency  $\eta$  of the cell, which goes from 9.33% to 21.41% for a thickness of 150 $\mu\text{m}$  of the base. Therefore, the optimum thickness for a polycrystalline silicon radial n/p junction solar cell is about 150 $\mu\text{m}$  for a wavelength of 1000nm (for  $R_b=50 \mu\text{m}$ ,  $S_b=2.10^2 \text{ cm/s}$ ,  $L_n=50 \mu\text{m}$ ,  $D_n=26 \text{ cm}^2/\text{s}$ ).

**Keywords** - Efficiency, Fill factor, Photocurrent-Photovoltage (J/V), Power-Photovoltage (P/V), Radial junction solar cell.

## 1. Introduction

The effects of climate change that we are experiencing today lead us more than ever to other sources of renewable energy to find solutions for the protection of human being and their environment. Among renewable energy sources, the most coveted is the sun because only one hour of radiation on the earth's surface would cover the annual energy needs of the entire planet earth [1]. However, optoelectronic devices designed to use this source face many challenges, which sum up to how to improve their performance and, at the same time, reduce their costs. In this quest to overcome the limitations, several studies have been carried out. Researchers have moved from classical horizontal junction silicon cells, [2] to vertical junction cells [3-5] and from planar junction cells [6-9] to radial junction cells [10,11] which is the subject of this article. In that cell, the illumination is done on the front face of the cell parallel to the junction, as depicted in Figure 1. While

remaining in the n/p junction technology, here is the geometrical configuration that is explored. Radial and planar junctions cells are classified as cylindrical cells [6, 11].

Particularly, the planar junction n+/p polycrystalline silicon-based semiconductor has been widely investigated. Among these studies, it is found that of Trabelsi et al. [8] which showed the optimum thickness of the cell is about 50 $\mu\text{m}$  to get the maximum available current and that the grain boundaries recombination becomes important when the thickness is greater than the diffusion length for a small cylindrical grain radius. That leads to a decrease in the photocurrent. Mbodji et al. [7] based their study on the effect of the cylindrical grain radius on the cell electrical parameters. When the radius increases, the photovoltage, photocurrent density and shunt resistance increase. Leye et al. [9] go beyond the geometrical effect on cell performances by studying the



effect of temperature. It is shown that when the temperature increases, the production efficiency of the cell is negatively influenced. However, the radial junction is less studied in cells with a thick base as classical polycrystalline silicon-based semiconductor except in nanowires solar cells where it has been widely investigated [11-15]. The radial configuration is preferred due to the multiple advantages that it presents. Comparative studies conducted on cubic and cylindrical solar cells have shown a slight improvement in photovoltaic parameters in favor of the cylindrical design [8]. In the same vein, simulation work carried out on cells in the case of nanowires has shown the advantage of the radial junction over a planar junction [11]. Thus, a cylindrical grain with a radial junction can combine these advantages in favor of the photovoltaic parameters. In view of this configuration, a reduction in the path of the photogenerated charge carriers is obtained when the solar cell is illuminated [13], resulting in a lower recombination rate. With this, the standard limits [16] can be reached with a reduction in the quantity and quality of the material. This will allow a substantial reduction in terms of the solar module cost [10].

As mentioned above, among few studies done on classical polycrystalline silicon-based semiconductor radial n/p junction solar cells, that is limited to the effect of the base thickness, radius and wavelength on the quantum efficiency and photocurrent density without mentioning the effect of the base thickness on the other electrical parameters. Therefore, the influence of grain size on polycrystalline silicon solar cells' performances with radial junctions remains less known, although studies exist for horizontal [2], vertical [3] and planar [8] junction configurations.

The goal of this work is, therefore, to carry out a theoretical study on polycrystalline silicon n/p radial junction solar cells to determine the influence of the base thickness on its electrical performance through modeling and simulation under monochromatic illumination in a static regime. Therefore, in this paper, it has been investigated the evolution of the short-circuit photocurrent ( $J_{phcc}$ ), open-circuit photovoltage ( $V_{phoc}$ ), form factor (FF), maximum power ( $P_{max}$ ), photovoltage ( $V_{phmax}$ ), photocurrent ( $J_{phmax}$ ), optimum load resistance ( $R_{op}$ ) and conversion efficiency when the thickness  $H$  of the base of the cell changes.

This paper is structured as follows: the theory showing the modelling of the single radial n/p junction with equations is done in section 2. In section 3, the simulation results and discussion are presented. And the conclusion is in section 4.

## 2. Theory

Our study model is shown in Fig. 1, which is a front-illuminated polycrystalline silicon-based semiconductor radial n/p junction photovoltaic cell. It consists essentially of

a n-doped emitter ( $10^{15} - 10^{17}$  atoms.cm<sup>-3</sup>) and a p-type base (with a doping rate equal to  $N_b=10^{16}$  atoms.cm<sup>-3</sup>) of radius  $R_b$  and thickness  $H$ . We have a space charge region (SCR) or depletion zone located between the emitter and the base. We admit to working in the assumption of the quasi-neutral base (Q.N.B), thus removing the crystal field [9].

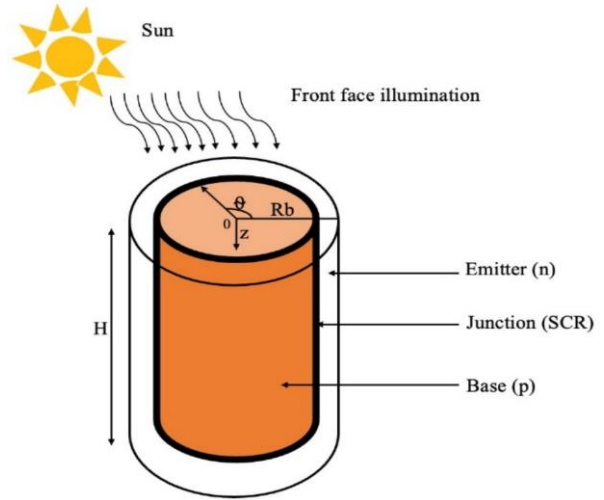


Fig. 1 Radial junction solar cell

We consider only the contribution from the base. The distribution equation of excess minority carriers in the base of the model (Fig. 1) is given by (1):

$$\frac{\partial \delta_n}{\partial t} = \frac{1}{e} \vec{\nabla} \cdot \vec{J}_n + G_n(z) - R_n(z) \quad (1)$$

$G_n(z)$  represents the minority carrier generation rate at the  $z$ -position. its expression for monochromatic illumination is [6]:

$$G_n(z) = \alpha(\lambda)(1 - R(\lambda))\phi_0 e^{-\alpha(\lambda)z} \quad (2)$$

Where  $\alpha(\lambda)$  and  $R(\lambda)$  represent the absorption coefficient and the monochromatic reflection coefficient of the corresponding material at a given wavelength, respectively.  $\phi_0$  is the monochromatic flux of incident photons.  $R_n(z)$  is the recombination rate of the minority carriers at the  $z$  coast and is written [3]:

$$R_n(z) = \frac{\delta_n(r,\theta,z,\lambda)}{\tau} \quad (3)$$

Starting from the magneto-transport equation and assuming that no field exists outside the space charge region and generation of carriers along  $\theta$  uniform given the symmetry, therefore, the carrier density is invariant by rotation of any angle  $\theta$ [8]. Thus, in the static regime ( $\frac{\partial \delta_n(r,\theta,z,\lambda)}{\partial t} = 0$ ) and applying the cylindrical coordinates, the continuity equation (1) is summarized in equation (4);

$$\frac{\partial^2 \delta_n(r,z,\lambda)}{\partial r^2} + \frac{1}{r} \frac{\partial \delta_n(r,z,\lambda)}{\partial r} + \frac{\partial^2 \delta_n(r,z,\lambda)}{\partial z^2} - \frac{\delta_n(r,z,\lambda)}{L_n^2} = - \frac{\alpha(\lambda)(1-R)\phi_0 e^{-\alpha(\lambda)z}}{D_n} \quad (4)$$

With  $D_n$  representing the diffusion coefficient in the base and  $L_n = \sqrt{D_n \tau}$  the charge carrier diffusion length. Equation (5) represents the general solution of equation (4) [6, 8]:

$$\delta_n(r, z, \lambda) = \sum_{k \geq 0} f(r, \lambda) \sin(C_k z) \quad (5)$$

$$\delta_n(r, z, \lambda) = \sum_{k \geq 0} \left( - \frac{2\alpha(\lambda)(1-R(\lambda))\phi_0 L_{nk}^2 C_k^2 [1+(-1)^{k+1} \exp(-\alpha H)]}{\left(\frac{2D_n}{S_f L_{nk}} I_0\left(\frac{R_b}{L_{nk}}\right) + I_0\left(\frac{R_b}{L_{nk}}\right)\right) (D_n(C_k^2 + \alpha^2)(C_k H - \sin(C_k H) \cos(C_k H)))} I_0\left(\frac{r}{L_{nk}}\right) + \frac{2\alpha(\lambda)(1-R(\lambda))\phi_0 L_{nk}^2 C_k^2 [1+(-1)^{k+1} \exp(-\alpha H)]}{D_n(C_k^2 + \alpha^2)(C_k H - \sin(C_k H) \cos(C_k H))} \right) \sin(C_k z) \quad (6)$$

With  $C_k$  defined by the transcendental equation (7),

$$C_k \cot a n(C_k H) = - \frac{S_b}{D_n} \quad (7)$$

$$\text{and} \quad \frac{1}{L_{nk}^2} = \frac{1}{L_n^2} + C_k^2 \quad (8)$$

$I_0$  is the Bessel function of 1<sup>ère</sup> modified species of order 0.

The boundary conditions posed are:

- at the emitter-base interface

$$\frac{\partial \delta_n(r,z,\lambda)}{\partial r} \Big|_{r=R_b} = - \frac{S_f}{2D_n} \cdot \delta_n(R_b, z, \lambda) \quad (9)$$

- on the back side

$$\frac{\partial \delta_n(r,z,\lambda)}{\partial z} \Big|_{z=H} = - \frac{S_b}{D_n} \cdot \delta_n(r, H, \lambda) \quad (10)$$

Where  $S_f$  is the dynamic velocity at the junction and  $S_b$  the recombination velocity at the backside of the cell.

- on the front side

$$\delta_n(r, z = 0, \lambda) = 0 \quad (11)$$

### 2.1. Photocurrent Density

The photocurrent density is determined based on Fick's law through the following expression:

$$J_{ph} = \frac{2qD_n}{R_b} \int_0^H \frac{-\partial \delta_n(r,z,\lambda)}{\partial r} \Big|_{r=R_b} dz \quad (12)$$

### 2.2. Photovoltage

The photovoltage is obtained from the Boltzmann relation.

Where  $C_k$  is an eigenvalue

The continuity equation final solution requires the determination of  $f(r, \lambda)$  and  $C_k$ , and this with using boundary conditions given below (Equations 9 and 10) and through the Bessel equations, equation (5) then becomes equation (6) representing the excess minority carriers in the base of the cell;

$$V_{ph} = V_T \ln \left[ 1 + \frac{1}{n_0} \int_0^H \delta_n(r = R_b, z, \lambda) (2\pi R_b) dz \right] \quad (13)$$

In this expression,  $V_T$  thermal voltage:  $V_T = \frac{K_B T}{q}$ ,  $n_0$

electron density at thermodynamic equilibrium:  $n_0 = \frac{n_i^2}{N_B}$ .  $n_i$

is the intrinsic electron concentration  $N_B$  is the base impurity doping rate, and  $K_B$  is the Boltzmann constant.

### 2.3. Electrical Power

The electrical power transferred to the external circuit by the base of the photocell is governed by equation (14):

$$P_{elec}(S_f) = V_{ph}(S_f) \cdot J_{ph}(S_f) \quad (14)$$

In this equation (14),  $J_{ph}(S_f)$  is the photocurrent density supplied by the cell to the load circuit and  $V_{ph}(S_f)$  the voltage across the photocell as a function of the dynamic speed.

### 2.4. Conversion Efficiency

Under monochromatic illumination, the conversion efficiency of a silicon solar cell is expressed in equation (15) [17]:

$$\eta = \frac{P_{max}}{P_{ab}} \quad (15)$$

Where,  $P_{ab} = \frac{\phi_0(\lambda) \cdot [1-\rho(\lambda)] \cdot h \cdot c}{\lambda}$  is the power of the absorbed light flux for monochromatic illumination,  $\phi_0(\lambda)$  the incident luminous flux in number of photons per  $cm^2/s$ ,  $\rho(\lambda)$  the reflection coefficient of the light wave on the front face of the photocell,  $h$  Planck's constant in  $J \cdot s$ ,  $c$  is the celerity of light in space in  $cm \cdot s^{-1}$  and  $\lambda$  the wavelength of the incident light in  $cm$ .

### 3. Results and Discussion

#### 3.1. Study of Photocurrent Density-Photovoltage ( $J/V$ ) and Power-Photovoltage ( $P/V$ ) Characteristics of the Cell

Fig. 2 and Fig. 3 show the profiles of the  $J/V$  and  $P/V$  characteristics of the cell for different values of the base thickness, respectively.

Fig. 2 shows that the photocurrent density remains maximum and almost constant at low photovoltage values. This situation remains prolonged with the increase of the base thickness  $H$ . Then we observe a brief decrease which ends up cancelling out at the neighborhood of the open circuit.

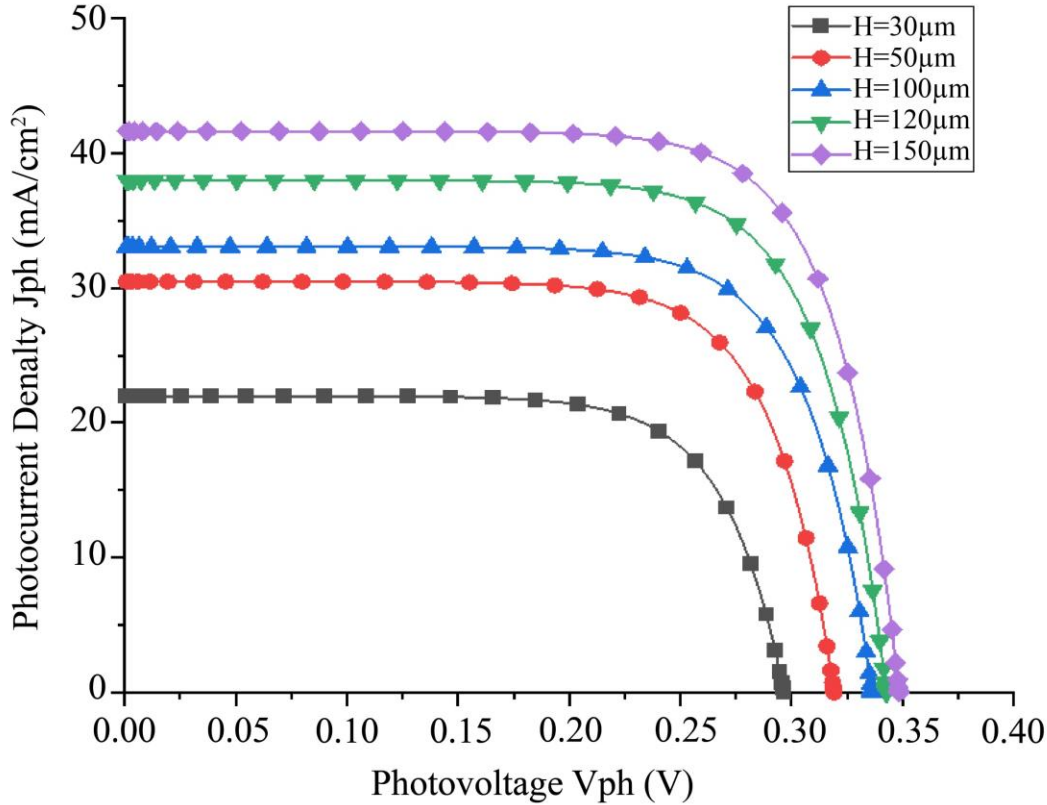


Fig. 2  $J/V$  characteristic profile for different values of the base thickness  $H$ ;  $S_b = 2.10^2$  cm/s,  $R_b = 50 \mu\text{m}$ ,  $\lambda = 1000$  nm,  $L_n = 50 \mu\text{m}$ ,  $D_n = 26$  cm<sup>2</sup>/s

Moreover, a clear enhancement of the photocurrent density and photovoltage is noticed, especially that of the short-circuit photocurrent density and the open-circuit photovoltage when the thickness  $H$  of the cell increases. i.e. from a thickness  $H$  of 30 to 150  $\mu\text{m}$ , the short-circuit photocurrent  $J_{phcc}$  goes from 21.989 to 41.161 mA/cm<sup>2</sup> while the open-circuit photovoltage  $V_{phoc}$  goes from 0.296 to 0.348 V (see Table 1), i.e. an increase of 87% for  $J_{phcc}$  against 17% for  $V_{phoc}$ . It follows, therefore, that the  $J_{phcc}$  is much more sensitive to the thickness  $H$  of the base than is the open-circuit photovoltage. This results in an augmentation in the shunt resistance, which characterizes a decrease in leakage currents [18].

Indeed, for a wavelength of 1000 nm, as is the case here, the absorption coefficient is low, and thus, the penetration depth is high [17, 19]. i.e. 1000 nm corresponds approximately to a penetration depth of about 160 $\mu\text{m}$  ( $1/\alpha$ ). Therefore, an increase in cell thickness contributes to an improvement in

light absorption. This increase induces an enlargement in the space of charge carrier movement as the collection of generated charge carriers is essentially along the lateral surface (radial structure). A smoother movement of the carrier flow at the junction is achieved, leading to a decrease in the recombination rate and thus involving an augmentation in the short circuit photocurrent density  $J_{phcc}$ . Also, the maximum distance travelled by these carriers to attain the junction and participate in the photocurrent remains unchanged for a given base radius.

The decrease of the rate of recombination through the increase of the thickness  $H$  is also at the work of the increase of the photovoltage, in particular that of the open-circuit photovoltage, which results from an increase of the accumulation of photogenerated carriers at the junction.

Fig. 3 shows the profiles of the  $P/V$  characteristic of the cell, highlighting the evolution of the maximum electrical power for different values of the base thickness  $H$ .

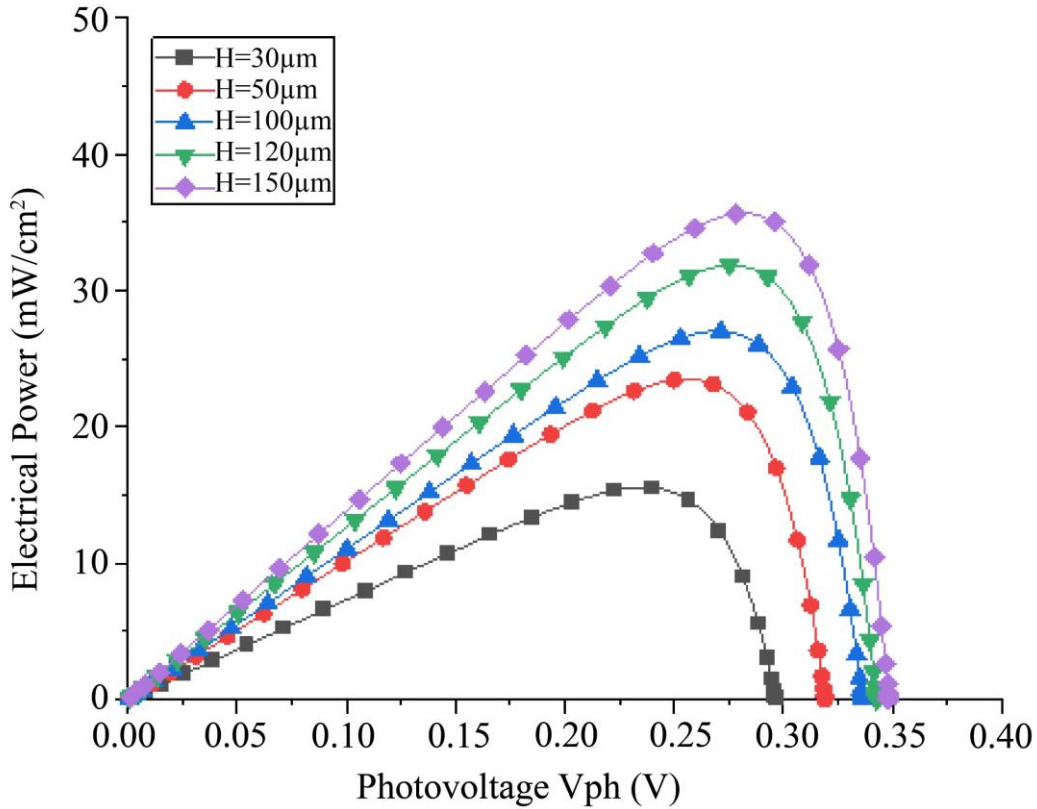


Fig. 3 P/V characteristic profile for different values of base thickness H; Sb = 2.10<sup>2</sup> cm/s, Rb = 50 μm, λ = 1000 nm, Ln = 50 μm, Dn = 26 cm<sup>2</sup> /s

In Fig. 3, each curve shows the same pace. From a thickness H of 30 to 150 μm,  $P_{max}$  it increases from 4.669 to 10.708 mW/cm<sup>2</sup> which is also observed at the level of  $V_{phoc}$  as highlighted above (see Table 1). The electric power increases with the photovoltage to reach a maximum value before decreasing and finally cancelling when the photovoltage reaches the  $V_{phoc}$ . In particular,  $P_{max}$  increases with increasing thickness H and tends slightly towards the open-circuit values; hence, an extension of  $V_{ph}$  with increasing  $P_{max}$ .

Indeed, beyond causing a decrease in volume recombination, as previously pointed out, an increase in the thickness H of the cell causes a rapid increase in electrical power at low values of the open circuit; i.e. the carriers arrive rapidly at the junction more than they cross it to participate in the photocurrent. The storage of the carriers is brief, which means that it is quickly achieved, taking with it the maximum power about the open circuit. The following paragraph consists of extracting the values of the electrical parameters of the cell according to the evolution of the thickness H of the base to appreciate its influence more.

### 3.2. Extraction of the Solar Cell Electrical Parameters from the J/V and P/V Characteristics

For this, we employ a technique that several different

authors have used [20]. This technique consists of plotting the curves of the J/V and P/V characteristics in the same reference frame, as shown in Fig. 4. Thus, from the curves obtained in Fig. 2 and Fig. 3, plotted in the same reference frame, we obtain the maximum values of the electrical power, the photovoltage and photocurrent density, the short-circuit photocurrent density and the open-circuit photovoltage.

Furthermore, with the values obtained above, the conversion efficiency, fill factor and optimum load resistance are obtained by applying formulas 15, 16 and 17, respectively;

$$FF = \frac{P_{max}}{J_{phc} \cdot V_{oc}} \quad (16)$$

$$R_{op} = \frac{V_{max}}{J_{phmax}} \quad (17)$$

The results obtained are recorded in Table 1 below. From this table, a clear influence of the base thickness H is observed on different photovoltaic parameters of the cell. By making a comparison with other studies carried out following the influence of the size of the grain on the electrical performances of a solar cell [20], for a radial junction cell, the increase in size is found in the increase of the thickness H of the base.

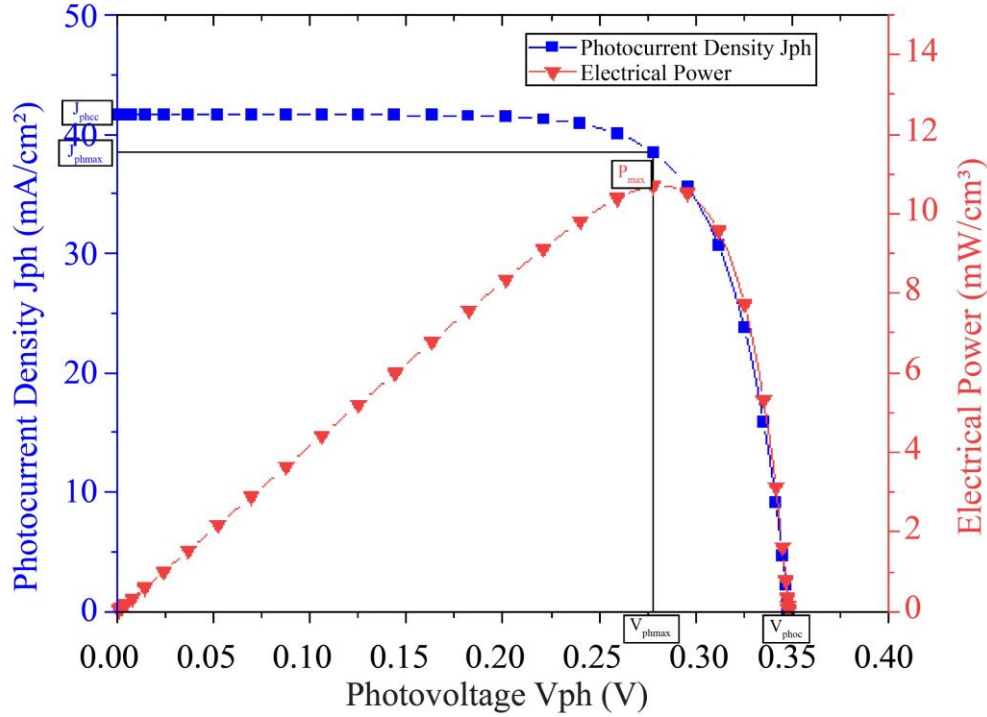


Fig. 4 Illustration of the extraction of electrical parameters

However, the optimal external load resistance  $R_{op}$  evolves inversely to the thickness  $H$  of the solar cell. It decreases while the base thickness increases. Indeed, the external load resistance is the resultant of the ratio between the maximum photovoltage and the maximum current density (equation 17) and is determined experimentally when it is close to the internal resistance of the cell at the point of maximum power; then, its decrease indicates an improvement (increase) of the photocurrent density. This proves that the

thickness  $H$  of the base remains favourable to the electrical performance of the cell, involving the improvement of the conversion efficiency, which passes from 9.33% for a thickness of 30 $\mu$ m to 21.41% for a thickness of 150 $\mu$ m (Table 1). Then, the optimal thickness for a polycrystalline silicon cell with radial junction is related to the depth of light penetration, i.e. the thickness  $H$  must be equal to approximately the latter ( $H \approx \frac{1}{\alpha}$ ). This result was also proved by Kayes in the case of nanowires solar cell [12].

Table 1. Electrical parameters of the solar cell for different values of the base thickness  $H$ ;  $R_b=50 \mu\text{m}$ ,  $S_b =2.102 \text{ cm/s}$ ,  $L_n=50 \mu\text{m}$ ,  $\lambda=1000 \text{ nm}$ ,  $D_n=26 \text{ cm}^2/\text{s}$

$H(\mu\text{m})$	30	50	100	120	150
$P_{max}(\text{mW}/\text{cm}^2)$	4.669	7.056	8.113	9.560	10.708
$V_{phmax}$	234.610	256.160	271.440	275.340	256.160
$J_{max}(\text{mA}/\text{cm}^2)$	19.905	29.890	29.890	34.724	37.694
$J_{phcc}(\text{mA}/\text{cm}^2)$	21.989	30.465	33.064	37.974	41.616
$V_{phoc}(\text{mV})$	296.730	319.24	336.24	342.73	348.39
FF(%)	71.550	72.550	72.97	73.450	73.850
$\eta$ (%)	9.338	14.112	16.226	19.120	21.416
$R_{op}(\Omega \cdot \text{cm}^{-2})$	11.780	9.300	9.080	7.9290	7.536

#### 4. Conclusion

This theoretical study allowed us to highlight the influence of the thickness  $H$  of the base of the radial n/p junction solar cell based on silicon polycrystalline on its electrical parameters. After the establishment of a continuity equation that suits our study model, we proceeded to its

resolution using Bessel's equations. This allowed us to obtain a final solution leading to the different expressions of electrical parameters of the cell. The study reveals an improvement in the photoconversion parameters of the cell when the thickness  $H$  of the base increases. This increase is much more perspective at the level of the photocurrent,

particularly the short-circuit photocurrent, with an increase of 87% noted when the thickness H of the base goes from 30 to 150  $\mu\text{m}$ , the short-circuit photocurrent  $J_{phc}$  goes from 21.989 to 41.161  $\text{mA}/\text{cm}^2$ . This will involve a decrease in load resistance and an improvement of the cell efficiency  $\eta$  from 9.33% to 21.41% for a base thickness of 150 $\mu\text{m}$ . Therefore, the increase in grain size of a radial junction is found in the increase of its base thickness H, and the optimum thickness for a polycrystalline silicon n/p radial junction cell is about

150 $\mu\text{m}$  for a wavelength of 1000nm (for  $R_b=50 \mu\text{m}$ ,  $S_b=2.10^2 \text{cm/s}$ ,  $L_n=50 \mu\text{m}$ ,  $D_n=26 \text{cm}^2/\text{s}$ ).

### Acknowledgment

The author wishes to express their gratitude to the International Scientific Program (ISP), University of Uppsala, Sweden, for financial support through the project BUF01.

### References

- [1] Xiaodong Wang, and Zhiming M. Wang, *High-Efficiency Silicon Solar Cells*, Physics, Materials, and Devices, Springer Series in Materials Science, vol. 190, 2014. [[CrossRef](#)] [[Google Scholar](#)] [[Publisher Link](#)]
- [2] M.M. Deme et al., "Influence of Illumination Incidence Angle, Grain Size and Grain Boundary Recombination Velocity on the Facial Solar Cell Diffusion Capacitance," *Journal of Renewable Energies*, vol. 13, no. 1, pp. 109-121, 2010. [[CrossRef](#)] [[Google Scholar](#)] [[Publisher Link](#)]
- [3] O. Mballo, B. Seibou, M. Wade, M. S. Diouf, and I. Ly, "Influence of the Depth base on the Electrical Parameters of a Parallel Vertical Junction Silicon Solar Cell under Polychromatic Illumination," *International Journal of Electrical Engineering*, vol. 4, no. 7, pp. 6-16, 2016.
- [4] Gokhan Sahin, and Genber Kerimli, "Effect of the Depth Base Along the Vertical on the Electrical Parameters of a Vertical Parallel Silicon Solar Cell in Open and Short Circuit," *Results in Physics*, vol. 8, pp. 257-261, 2018. [[CrossRef](#)] [[Google Scholar](#)] [[Publisher Link](#)]
- [5] Youssou Traore et al., "AC Recombination Velocity in the Back Surface of a Lamella Silicon Solar Cell under Temperature," *Journal of Modern Physics*, vol. 10, no. 10, pp. 1235-1246, 2019. [[CrossRef](#)] [[Google Scholar](#)] [[Publisher Link](#)]
- [6] S. Elnahwy and N. Adeeb, "Exact Analysis of a Three-Dimensional Cylindrical Model for a Polycrystalline Solar Cell," *Journal of Applied Physics*, vol. 64, no. 10, pp. 5214-5219, 1988. [[CrossRef](#)] [[Google Scholar](#)] [[Publisher Link](#)]
- [7] Assane Diouf, Amadou Diao, and Senghane Mbodji, "Effect of the Grain Radius on the Electrical Parameters of an N+/P Polycrystalline Silicon Solar Cell Under Monochromatic Illumination Considering the Cylindrical Orientation," *Journal of Scientific and Engineering Research*, vol. 5, no. 2, pp. 174-180, 2018. [[Publisher Link](#)]
- [8] Abdessalem Trabelsi, Abdelaziz Zouari, and Adel Ben Arab, "Modeling of Polycrystalline N +/ P Junction Solar Cell with Columnar Cylindrical Grain," *Journal of Renewable Energies*, vol. 12, no. 2, pp. 279-297, 2009. [[CrossRef](#)] [[Google Scholar](#)] [[Publisher Link](#)]
- [9] Serigne Ndiangue Leye et al., "Analysis of T-Coefficients Using the Columnar Cylindrical Orientation of Solar Cell Grain," *Smart Grid and Renewable Energy*, vol. 9, no. 3, pp. 43-56, 2018. [[CrossRef](#)] [[Google Scholar](#)] [[Publisher Link](#)]
- [10] Erik C. Garnett et al., "Nanowire Solar Cells," *Annual Review of Materials Research*, vol. 41, no. 1, pp. 269-295, 2011. [[CrossRef](#)] [[Google Scholar](#)] [[Publisher Link](#)]
- [11] Brendan M. Kayes, Harry A. Atwater, and Nathan S. Lewis, "Comparison of the Device Physics Principles of Planar and Radial P-N Junction Nanorod Solar Cells," *Journal of Applied Physics*, vol. 97, no. 11, 2005. [[CrossRef](#)] [[Google Scholar](#)] [[Publisher Link](#)]
- [12] Brendan Kayes et al., "Radial PN Junction, Wire Array Solar Cells," *33<sup>rd</sup> IEEE Photovoltaic Specialists Conference*, San Diego, CA, USA, 2008. [[CrossRef](#)] [[Google Scholar](#)] [[Publisher Link](#)]
- [13] Dayan Ma et al., "A Novel Model of Mono-Crystalline Silicon P-N Homojunction," *The European Physical Journal Applied Physics*, vol. 82, no. 1, pp. 1-7, 2018. [[CrossRef](#)] [[Google Scholar](#)] [[Publisher Link](#)]
- [14] Vidur Raj et al., "High-Efficiency Solar Cells from Extremely Low Minority Carrier Lifetime Substrates Using Radial Junction Nanowire Architecture," *American Chemical Society Nano*, vol. 13, no. 10, pp. 12015-12023, 2019. [[CrossRef](#)] [[Google Scholar](#)] [[Publisher Link](#)]
- [15] Vidur Raj, Hark Hoe Tan, and Chennupati Jagadish, "Axial vs Radial Junction Nanowire Solar Cell," *Asian Journal of Physics*, vol. 28, no. 7-9, pp. 719-746, 2019. [[Google Scholar](#)] [[Publisher Link](#)]
- [16] William Shockley, and Hans J. Queisser, "Detailed Balance Limit of Efficiency of P-N Junction Solar Cells," *Journal of Applied Physics*, vol. 32, no. 3, pp. 510-519, 1961. [[CrossRef](#)] [[Google Scholar](#)] [[Publisher Link](#)]
- [17] A. Correa, "Modeling of Recombination at the Interfaces of a Polycrystalline Silicon Solar Cell in Steady State," 3<sup>rd</sup> Cycle Thesis, Université Cheikh Anta Diop de Dakar, Senegal, 1996. [[Google Scholar](#)]
- [18] W.C. Benmoussa, S. Amara, and A. Zerga, "Comparative Study of Models of the Current-Voltage Characteristic of a Monocrystalline Silicon Solar Cell," *Renewable Energy Review*, pp. 301-306, 2015. [[Google Scholar](#)] [[Publisher Link](#)]
- [19] J. Gervais, "Measurement of the Optical Absorption Coefficient in P-Type Multicrystalline Silicon for Solar Photocells," *Journal de*

*Physique III*, vol. 3, no. 7, pp. 1489-1495, 1993. [[CrossRef](#)] [[Google Scholar](#)] [[Publisher Link](#)]

- [20] M. Savadogo et al., “3-D Modeling of Grains Sizes Effects on Polycrystalline Silicon Solar Cell Under Intense Light Illumination,” *Sylwan*, vol. 161, pp. 2-13, 2017. [[Google Scholar](#)] [[Publisher Link](#)]